Changes in spherical aberration after lens refilling with a silicone oil

Wong, Kwok-Hoi; Koopmans, Steven A.; Terwee, Thom; Kooijman, Aart C.

Published in:
Investigative ophthalmology & visual science

DOI:
10.1167/iovs.06-0352

Publication date:
2007

Changes in Spherical Aberration after Lens Refilling with a Silicone Oil

Kwok-Hoi Wong,[1] *Steven A. Koopmans,*[1] *Thom Terwee,*[2] *and Aart C. Kooijman*[1]

Purpose. It may be possible to restore accommodation to presbyopic human eyes by refilling the lens capsular bag with a soft polymer. In the present study, optical changes were measured that occurred in a pig eye model after the refilling of the capsular bag.

Methods. The optical power and spherical aberration in 10 isolated pig lenses were measured under different conditions. They were first determined by using a scanning laser ray-tracing technique over an effective pupil size of 6 mm. Second, the contours of the anterior and posterior lens surface were photographed, and a mathematical ray-tracing was performed by using a polynomial fit through the digitized surface contours, to determine optical power and spherical aberration. Third, the lenses were refilled with a silicone oil until their preoperative lens thickness was reached, and scanning laser ray-tracing, contour photography, and mathematical ray-tracing were repeated. Comparisons between the measurements were made to determine how the change from a gradient refractive index to a homogeneous refractive index influenced spherical aberration. The influence of the change in lens contour on spherical aberration after lens refilling was also studied.

Results. The natural lenses had a higher lens power than the refilled lenses (49.9 ± 1.5 D vs. 36.8 ± 1.5 D; $P < 0.001$). Moreover, there was a change in sign from negative spherical aberration before lens refilling (−3.6 D) to positive spherical aberration after lens refilling (7.9 D; $P < 0.001$). The comparison between scanning laser ray-tracing of the natural lens and mathematical ray-tracing of the photographed surface contours of the natural lens to determine the effect of refractive index substitution (i.e., replacement of a gradient refractive index by a homogeneous refractive index) showed a significant change in spherical aberration from −3.6 ± 2.0 to 11.0 ± 2.1 D ($P < 0.001$). The change in lens contour did not result in a significant change in spherical aberration ($P = 0.08$) before and after lens refilling with an equal refractive index.

Conclusions. The lower lens power of refilled pig lenses compared to natural lenses was due to the lower refractive index of the refill material. Refilling pig lenses with the silicone oil used in this study resulted in an increase in spherical aberration. This increase was mainly caused by the change from a gradient refractive index to a homogeneous refractive index. The change in lens curvature after lens refilling did not result in an increase in spherical aberration. The influence of lens refilling on spherical aberration of human lenses must be determined in similar experiments in human eyes. (*Invest Ophthalmol Vis Sci.* 2007;48:1261–1267) DOI:10.1167/iovs.06-0352

Surgical restoration of accommodation after the onset of presbyopia has received considerable attention lately. To the authors' knowledge, however, none of the published procedures are capable of restoring more than 1 D of accommodation in the living human eye. Because presbyopes usually need reading glasses with a power of 2 to 3 D, an accommodative amplitude of 1 D is insufficient for prolonged reading.

According to the classic Helmholtz theory of accommodation,[1] the emmetropic eye is focused for distance when the ciliary muscle is relaxed. Under this condition, the zonular fibers, which are attached to the periphery of the lens, have a resting tension that maintains the lens in a relatively flattened state. On accommodation, the ciliary muscle contracts, causing a reduction in the ciliary body diameter and a release of the zonular fiber tension. This action allows young lenses to regain their unstretched shape, which is characterized by an increase in the anterior and posterior lens curvature. This results in an increase in lens power, and objects near the eye are focused on the retina. All the structures involved in accommodation (lens capsule, lens nucleus, and cortex, zonular fibers, ciliary muscle, and choroid) show age-related changes that may explain the onset of presbyopia at the approximate age of 45 years. Many investigators, however, consider a hardening of the lens nucleus and cortex to be the most important factor causing presbyopia. This seems to be an intuitively logical explanation, since the lens changes its shape during accommodation. Pau and Kranz[2], for example, described the simultaneous increase in lens sclerosis and decrease in accommodative ability. Heys et al.[3] showed that the increasing stiffness of the human lens with age is most pronounced in the nucleus. Further, by placing lenses on a rapidly rotating table, Fisher[4] demonstrated that older lenses are more resistant to deformation than are younger lenses. Glasser and Campbell[5] established that older lenses, when exposed to equatorial stretching forces, show less change in focal length than do younger lenses. Thus, if the lens nucleus and cortex are responsible for presbyopia, then replacement of the hardened lens substance by a suitable soft, transparent polymer should restore the accommodative range.

Kessler[6] was the first to describe a surgical method to replace the contents of the capsular bag of the crystalline lens with a soft refill material. He removed the lens cortex and nucleus by means of a small capsulorrhexis and injected a flexible polymer into the bag. He then used a plug to prevent leakage of the polymer from the capsular bag. Later in vitro studies of refilled human eyes[7] and in vivo studies of nonhuman primate eyes[8–10] found accommodative changes in the refilled lenses, indicating the potential for this procedure. Replacement of the natural lens content by a silicone polymer, however, influences the optical properties of the lens. To begin with, the gradient refractive index that exists in the natural lens is changed to a homogeneous refractive index. Studies have shown that such a change in refractive index clearly influences spherical aberration. For example, the opti-

From the [1]Department of Ophthalmology, University Medical Center Groningen, University of Groningen, Groningen, The Netherlands; and [2]Advanced Medical Optics, Groningen, The Netherlands.

Submitted for publication March 30, 2006; revised September 15, 2006; accepted December 26, 2006.

Disclosure: **K.H. Wong**, Advanced Medical Optics (F); **S.A. Koopmans**, Advanced Medical Optics (C, F); **T. Terwee**, Advanced Medical Optics (P); **A.C. Kooijman**, None

The publication costs of this article were defrayed in part by page charge payment. This article must therefore be marked "*advertisement*" in accordance with 18 U.S.C. §1734 solely to indicate this fact.

Corresponding author: Kwok-Hoi Wong, Department of Ophthalmology, University Medical Center Groningen, University of Groningen. Hanzeplein 1, 9713 GZ Groningen, The Netherlands; kochoi@yahoo.com.

cal analysis by Smith et al.[11] showed that the gradient refractive index is responsible for the negative spherical aberration of the crystalline lens, whereas Koopmans et al.[7] demonstrated that refilled ex vivo human lenses had predominantly positive or zero spherical aberration, but never the negative spherical aberration of natural human lenses. These latter researchers did not, however, quantify the spherical aberration. A second optical factor that changes after lens refilling and that could influence spherical aberration is the curvature of the surfaces of the refilled lens. It is not yet clear how the lens curvature changes after the lens capsule has been refilled. Lens curvature is influenced by the amount of material that is injected into the capsular bag.[12] To make a useful comparison between the optical properties of natural and refilled lenses, it seems logical to compare natural lenses with lenses that have been filled to a level that re-establishes the original lens dimensions. The purposes of the present study were to establish the amount of spherical aberration before and after lens refilling and to determine whether the change in spherical aberration was caused by the change in lens curvature or by the change from a gradient refractive index to a homogeneous refractive index. To do this, the optical properties of 10 pig lenses were measured before and after lens refilling. The use of lenses from a species with a sturdy lens capsule (e.g., from a pig) was advantageous because several measurements and associated manipulations were needed for each lens. Furthermore, pig eyes were easily available. Lens thickness is a parameter that can be measured and influenced during surgery, and so the lenses were refilled to a predetermined thickness similar to that of the natural lens.

Materials and Methods

Ten eyes from 6-month-old pigs were obtained from a local abattoir. The eyes were enucleated immediately after death, kept in a saline solution consisting of 8 g/L NaCl, 0.4 g/L KCl, 1 g/L glucose, 2.38 g/L HEPES, and 0.1 g/L Na_2HPO_4 and stored in a refrigerator at 5°C until the experiments started (i.e., within 24 hours after enucleation).

Measurement of Natural Lens Thickness

When a natural lens is removed from an eye, its thickness may be altered. Therefore, the natural lens thickness was measured in four conditions. The tissues were regularly wetted with saline during the experiments.

Condition 1. The eye was positioned in a cup with the cornea facing upward. The extraocular muscles and conjunctiva were removed with scissors. A 10-mHz ultrasound A-scan probe (A-5500; Sonomed, Lake Success, NY) was used to measure the thickness of the lens. The probe was manually held perpendicular to the cornea until maximum echographic signal peaks of the anterior and posterior surfaces of the lens were obtained. Three measurements were taken, and the mean thickness was used.

Condition 2. Guided by a surgical microscope, a paracentesis was made in the cornea, and an anterior chamber maintainer (BD Biosciences, Oxford, UK) connected to an infusion bottle filled with saline was inserted into the eye. The physiological intraocular pressure (8 mm Hg) of a living pig was simulated by hanging the bottle of the saline 11 cm above the eye.[13] In this situation, the thickness of the lens was measured again with A-scan ultrasonography.

Condition 3. The cornea and the iris were removed. The ciliary body was then separated from the anterior sclera by blunt dissection. The anterior sclera was cut away to expose the ciliary body and the anterior choroid. Again, the thickness of the lens was measured with A-scan ultrasonography.

Condition 4. The lens-zonula-ciliary body apparatus was mounted in a plastic ring. The ring[7] with an inner diameter of 33 mm, was placed around the exposed choroid. Four sutures (8-0 virgin silk) were knotted to the ciliary body at the 12-, 3-, 6-, and 9-o'clock positions and threaded through four corresponding holes in the ring. The sutures were then immobilized by placing small plugs in the holes of the ring. The tension on the sutures was adjusted individually to make sure that the ciliary body remained unstretched and the sutures taut. Because the sutures were attached to the ciliary body, the forces on the sutures would did not directly affect the properties of the lens. Using a similar setup with a human lens in the same plastic ring, Koopmans et al.[7] showed that changes in lens power start to occur after 0.8 mm of stretching. Because the sutures were never stretched in our experiments, the minimal changes in tension should not have affected the optics of the lenses. After applying the sutures, a circumferential cut was made through the choroid in the region of the ora serrata to separate the anterior segment tissue from the posterior segment of the eye. The anterior segment tissue comprises the ciliary body, the ciliary muscle, the lens and the zonular complex. The plastic ring with the anterior segment was then lifted carefully and the remaining vitreous adhesions to the posterior segment were cut. The posterior segment was left in its place in the cup as a support. After the vitreous cuts were made, the anterior segment was placed back on the posterior segment in the cup and submerged in saline. Lens thickness was measured again using A-scan ultrasonography.

A sonic speed of 1704 m/s was used for the A-scan ultrasonography. This value was determined from the mean thicknesses of the lenses calculated from lens contour photography and measured by A-scan ultrasonography at room temperature.

Measurement of Focal Length

A scanning laser instrument[5] was used to measure the focal length of the lens (Fig. 1A). The ring containing the tissue was mounted vertically in a holder that was placed in a rectangular, saline-filled glass tank measuring 24 × 10 × 10 cm, with the anterior surface of the lens facing the laser beam. We assumed that the optical axis of a lens in this position was horizontal and parallel to the incident laser beams. The location of the optical axis of the lens was defined by the laser beam passing through the lens with the smallest slope difference and vertical displacement between incident and exiting beam. The saline solution was slightly clouded with coffee creamer, to visualize the laser beam passing through the solution. The lens was scanned vertically with a 5-mW HeNe laser beam (633 nm; 0.81 mm in diameter; model 1125; JDS Uniphase, Manteca, CA) by shifting the vertical position of a mirror on an *x-y* stage (model UTM25PP1HL; Newport, Irvine, CA) that was driven by a computer-controlled stepper motor (model MM3300; Newport). This stepper motor allowed the laser beam to be moved and positioned with an accuracy of approximately 12 μm. The horizontal and vertical displacement of the glass tank could be adjusted manually to make the laser coincide with the optical axis of the lens by estimation. A video camera (model XC77; Sony, Tokyo, Japan) viewed the glass chamber from the side. The laser beam was clearly visible in the slightly clouded saline solution. The laser beam position was recorded by the camera and displayed on a computer screen.

The incident and exiting pathways of the laser beam passing through the lens were digitized with image-processing software (Optimas, v6.5; Media Cybernetics, Silver Spring, MD). This program calculated the positions of the incident and exiting pathways and the slopes of the laser beams. Whenever the slope difference and the vertical displacements between the incident and exiting beams were smallest, the laser beam was deemed to coincide with the optical axis of the lens. During vertical lens scanning, the camera recorded the incident and exiting laser beams in the vertical meridional plane. The recorded beam paths were then reconstructed to calculate the lens power. Each vertical lens scan covered a distance of 6 mm in 51 discrete steps, from 3 mm above to 3 mm below the optical axis. Two scans of the natural lens and two scans of the refilled lens were performed for each lens. This procedure is called scanning laser ray-tracing (SLRT).

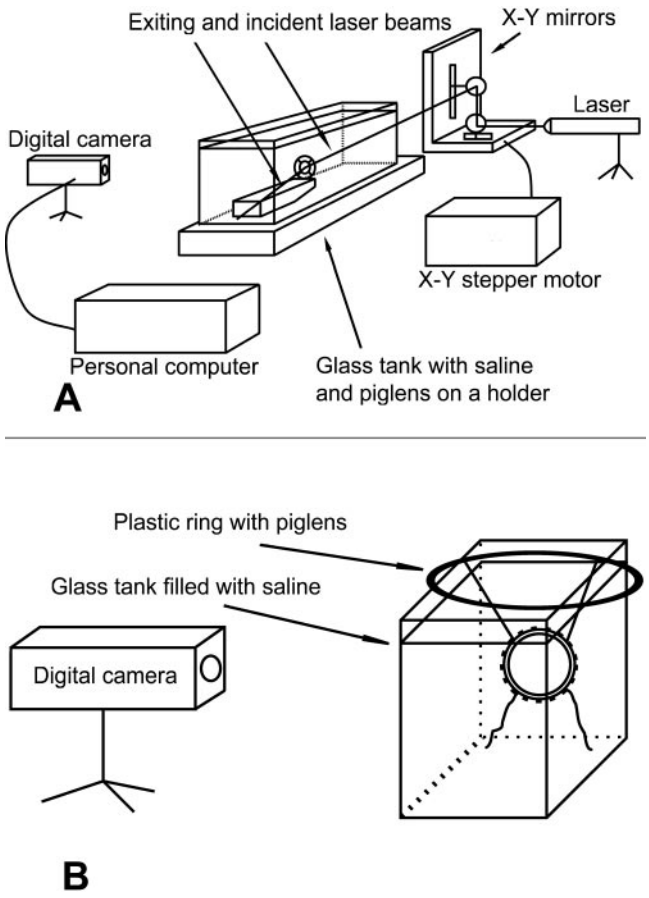

FIGURE 1. **(A)** Scanning laser setup for measuring the focal length and spherical aberration of the lens. **(B)** Contour photography setup to assess anterior and posterior radii of the lens.

Measurement of Anterior and Posterior Radius

The anterior and posterior radii of the lenses were assessed with digital lens surface contour photography. A rectangular glass tank with a volume of $10 \times 5 \times 5$ cm was filled with saline solution. The glass tank was placed on a revolving stand equipped with a circular scale graduated in 1° steps. A monochrome video camera (CV-M50; JAI, Yokohama, Japan) equipped with a macro lens (Cosmicar 75 mm; Pentax, Hamburg, Germany) was installed 30 cm in front of the glass tank. The video images were fed to a personal computer. The pixel-to-millimeter conversion was calculated from a picture of a steel calibration ball (0.5 in. in diameter), that was placed in the glass tank at the position where the pig lens would be photographed. The two inferior sutures were detached from the plastic ring, whereas the top of the lens remained attached via the other two sutures. The ring was then placed flat on top of the glass tank, so that the lens could hang freely and vertically in the saline solution (Fig. 1B). The lens was photographed with the optical axis perpendicular to the axis of the camera to determine the anterior and posterior surface contours.

To do this, the optical axis was first positioned perpendicular to the axis of the camera, as judged by observation. Then, a picture was taken and the area within the lens contour was determined using image-processing software (Optimas; Media Cybernetics). The lens was rotated in 5° steps until the smallest area within the lens contours could be determined. At this time, the optical axis of the lens was considered to be perpendicular to the camera axis. Four pictures of the lens were then taken. The glass tank containing the lens was rotated 180° between every picture so that each side of the lens was photographed twice. The digital image files were processed with custom image-processing software (using MatLab ver. 6.0; The MathWorks, Natick, MA). After the lens contours were detected, a circle was fitted, using a least-squares method, to the central 6-mm chord span of the anterior and posterior lens surfaces to determine the radius of curvature. The software corrected for the tilt of the lens: the position of the optical axis was defined by the line passing through the centers of the two circles fitted to the anterior and posterior surface contours.

Lens Refilling: The Surgical Procedure

After SLRT and lens contour photography, the two detached sutures were reattached to the plastic ring, again without excess tension or slack. The plastic ring was repositioned on the cup on the remnants of the bulbus which supported the lens in the ring. With the aid of a surgical microscope, the anterior capsule was punctured with a 27-gauge needle in the periphery of the lens. A minicircular capsulorrhexis of 1 to 1.5 mm in diameter was then created with appropriate forceps. The lens substance was aspirated manually with an 18-gauge cannula connected to a 10-mL syringe by an extension tube. A 2.7 mm diameter silicone plug was inserted into the capsular bag to prevent leakage. Silicone oil (AMO, Groningen, The Netherlands) was injected into the capsular bag by using a 5-mL syringe with a 25-gauge cannula. Before injection, the oil was briefly exposed to a vacuum to remove any air bubbles. The end point for refilling of the lens capsule was the same axial thickness of the natural lens in the plastic ring, within a range of ± 0.1 mm (the accuracy of A-scan ultrasonography[14]). Koopmans et al.[12] showed that refilling the pig lens to 100% of its original volume results in a lens thickness of approximately 7.0 mm. This is approximately the axial thickness of the lenses we used in the present study.

First, the capsular bag was refilled to the desired thickness by estimation. Then, the lens thickness was measured by A-scan sonic velocity set at 1066 m/s. We had established this sonic speed in the silicone oil by measuring a 10-mm cylinder of material with the A-scan at room temperature. If the lens was too thin, the cannula was reintroduced, and more material was added. If the lens was too thick, oil was removed by gently depressing the silicone plug and allowing some oil to escape. Excess oil was removed from the surface of the lens by flushing with saline. During refilling and removal of the oil from the surface of the lens, care was taken not to inject air bubbles or saline into the capsule.

SLRT and lens contour photography of the refilled lens were repeated as described for the natural pig lens. Because the specific gravities of the natural pig lens (1.03 g/mL) and the silicone oil (1.05 g/mL) used in this experiment were practically the same,[12] no difference in the state of stretch or fixation was expected when these lenses were immersed in the saline solution.

Silicone Oil

Usually, polymerizing materials are used for refilling lens capsules.[6–10] In the present study we used a nonpolymerizing silicone oil so that our measurements could be repeated at various degrees of lens refill without introducing a bias due to an ongoing polymerization process. This silicone oil has a refractive index of 1.42 and a viscosity of 1750 cP.

Analysis of the Data

Refractive Power of the Lens. To determine the refractive power of the natural and refilled lenses, we calculated the focal length of the lenses from the SLRT data using computer software (MatLab, ver. 6.0; The MathWorks). The intersecting points of the incident and exiting beams were calculated for each of the 51 beam pairs. Intersection points with coordinates in excess of 3 SD of the average intersection point were eliminated from the data set. A straight vertical line was then fitted through the remaining points and assumed to represent the principal plane of the lens. As noted earlier, the optical axis of the lens was defined as the beam passing through the lens with the smallest slope difference and vertical displacement between incident and exiting beams. The focal point of the lens was located by a fitting procedure.[7] To do this, we calculated the angles between the exiting

beams and the radius of the circle (centered on the optical axis) where the light rays intersected the perimeter of the circle. In conjunction with the fitting procedure, the center of the circle was shifted along the optical axis until the squared sum of these angles reached its minimum. At this time, the position of the center of the circle represented the focal point of the lens. The distance between the principal plane and the center of the circle, by definition, was the focal length. The refractive power of the lens could then be calculated.

Spherical Aberration. The spherical aberration was determined by fitting fourth-order polynomials to the intersections of the exiting beams with the optical axis as a function of scan diameter (Fig. 2). The difference between the average lens power at 3 mm above and below the optical axis and at the center of the lens gives the extent of the spherical aberration of the lens in diopters. Lens power at the center of the lens was obtained by using the solution of the polynomial at zero distance from the optical axis.

Mathematical Ray-Tracing. To determine the influences of the contour changes of the lens and the change from a gradient refractive index to a homogeneous refractive index on refractive power and spherical aberration, we used mathematical ray-trace software (MatLab ver. 6.0; The MathWorks). The program fitted a 10th-order polynomial to the lens contour data from the lens contour photographs and calculated the refraction of 51 parallel light rays evenly distributed over a 6-mm aperture through the contour, assuming a homogeneous refractive index within the lens. From these data the focal length and spherical aberration were calculated similar to the SLRT method. This method was called mathematical ray-tracing (MRT).

The equivalent refractive index of the natural pig lens was needed to compare between the data obtained by MRT and SLRT in natural pig eyes. The equivalent refractive index was established as the refractive index at which the mean refractive power in MRT of natural lenses equaled that of the mean refractive power obtained with the SLRT method. This equivalent refractive index (1.4686) was then used for subsequent calculations.

Statistical Analysis

The two-sided Student's *t*-test was used for the comparisons between the conditions.

Results

With the aid of A-scan ultrasonography, all the lenses were refilled successfully to the thickness of the natural lenses in condition 4. The mean thickness ± SD of both the natural lenses in condition 4 and the refilled lenses was 7.4 ± 0.1 mm (range, 7.2–7.5 mm). No silicone oil leaked from the capsule after refilling or during the measurements. Figure 3 shows the thickness of the lenses during the different stages of the experiment. The mean thickness of the lenses was 7.4 ± 0.1 mm in the untouched eye, 7.0 ± 0.1 mm when the eye was pressurized, 7.3 ± 0.1 mm after the cornea and the scleral ring were removed, and 7.4 ± 0.1 mm when the lens was attached to the plastic stretchring.

The minimum and maximum vertical deviations of the laser beam passing through the optical axis in SLRT were −0.26 and 0.10 mm, respectively. When 7.4 mm was used as the mean thickness of the lenses, the mean tilt of the lenses was calculated to be −0.08 ± 0.8° (range: −2.0–0.8°). The mean ± SD of the error of the fitting procedure according to a least-squares method through the surface contours of the lenses was ± 0.0003 mm (range, 0.0001 and 0.0007 mm). Table 1 shows the lens powers and spherical aberrations of the natural and refilled lenses as measured by SLRT and of the photographed contours of the natural and refilled lenses as measured by MRT.

The following comparisons were made between our datasets.

Comparison A

Datasets from SLRT through the natural and the refilled lenses were compared, showing the differences in refractive power

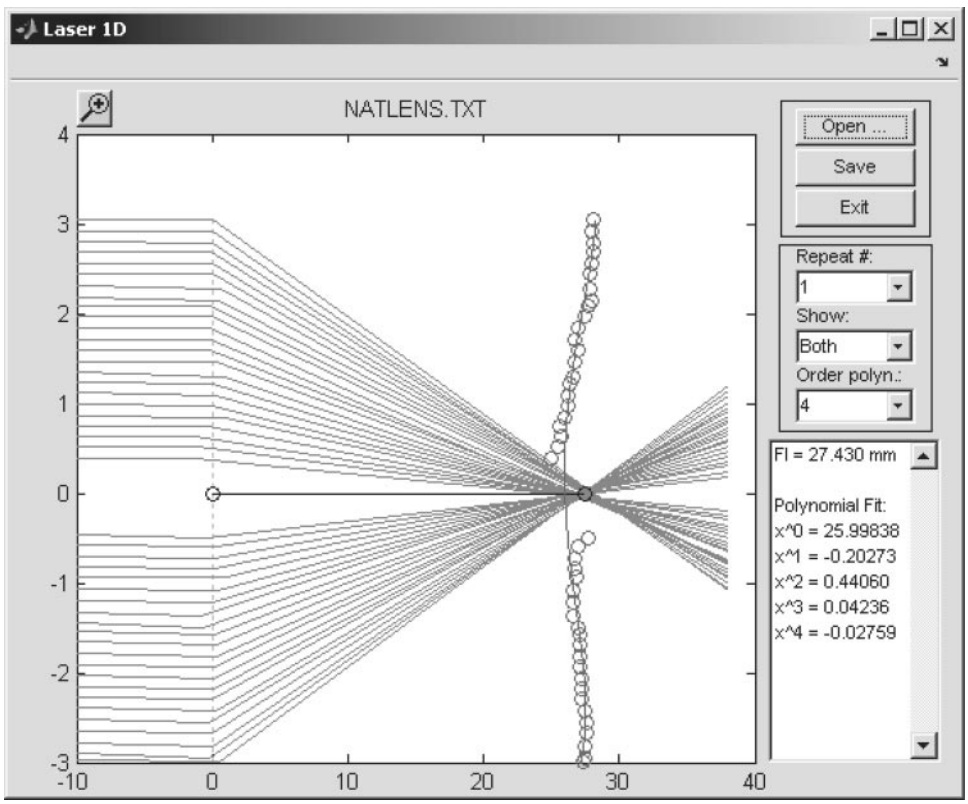

Figure 2. Reconstruction of a scan of a natural pig lens. *Vertical line* at the origin of the horizontal axis: principle plane of the lens; (○) horizontal position where each exiting beam intersects with the optical axis, and the vertical position where the incident beam meets the lens. A fourth-order polynomial was fitted to these points to determine the spherical aberration.

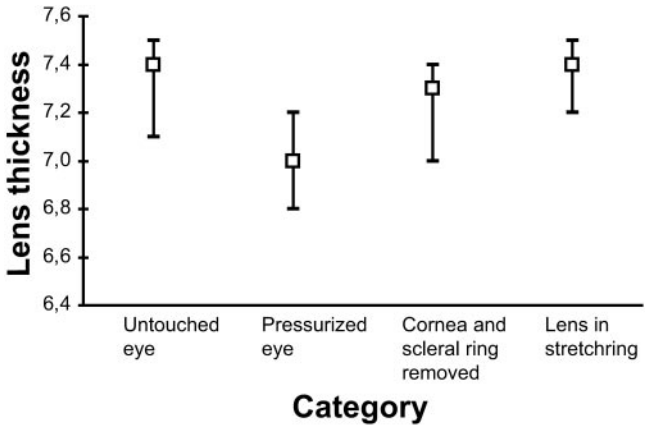

FIGURE 3. Natural lens thickness (mean + range) in the consecutive stages of pig eye preparation.

and spherical aberration between the natural and refilled lenses. The natural lenses had a mean refractive power of 49.9 ± 1.5 D and a negative spherical aberration of −3.6 ± 2.0 D. The refilled lenses had a lower mean refractive power (36.8 ± 1.5 D) and a positive spherical aberration of 7.9 ± 2.3 D. The differences in power and spherical aberration between the natural and the refilled lenses were significant (both $P < 0.001$).

Comparison B

Datasets from SLRT through the refilled lenses were compared with those from MRT of the photographed surface contours of the refilled lenses. The refractive index in MRT was set at 1.42. The mean refractive power and spherical aberration of the refilled lenses measured using SLRT were 36.8 ± 1.5 and 7.9 ± 2.3 D, respectively. MRT of the surface contours of the refilled lenses showed the refractive power and spherical aberration to be 36.7 ± 1.6 D and 8.6 ± 1.4 D, respectively. As expected, the differences between the two groups with regard to refractive power ($P = 0.89$) and spherical aberration ($P = 0.42$) were not significant.

Comparison C

Datasets from SLRT of the natural lenses were compared with those of MRT of the photographed surface contours of the natural lenses. The equivalent refractive index of the natural pig lens (1.4686) was used in MRT. This equivalent refractive index was approached by equalizing the refractive power (49.9 D) in MRT to the refractive power in SLRT. This comparison shows the influence of the refractive index substitution (i.e., a gradient refractive index is replaced by an equivalent homogeneous refractive index) on spherical aberration. As a result of our method to determine the equivalent refractive index, the mean refractive powers of the lenses in both datasets were equal (49.9 ± 0.2 D, $P = 0.99$). The mean spherical aberration of the natural lenses measured using SLRT was −3.6 ± 2.0 D. With the equivalent homogeneous refractive index, this aberration was +11.0 ± 2.1 D using MRT of the photographed surface contours of the natural lenses. The change in spherical aberration after the substitution of the gradient refractive index was significant ($P < 0.001$).

Comparison D

Datasets from MRT of the photographed lens surface contours before and after refilling were compared. The same equivalent homogeneous refractive index of 1.4686 was used in both groups to show the influence of surface contour changes after lens refilling on refractive power and spherical aberration. The mean refractive power and spherical aberration of the natural lenses were 49.9 ± 1.6 and 11.1 ± 2.1 D, respectively, if they had an equivalent homogeneous refractive index, whereas those of the refilled lenses were 55.6 ± 2.6 and 13.0 ± 2.4 D, respectively. The change in lens surface contours after refilling induced a significant increase in refractive power ($P < 0.001$), but not in spherical aberration ($P = 0.08$).

Comparison E

The radii of the anterior and posterior surface contours before and after refilling were compared by using lens surface contour photography. They became smaller after lens refilling. The mean anterior radius changed from 7.08 ± 0.35 to 6.30 ± 0.15 mm, the mean posterior radius changed from 5.08 ± 0.14 to 4.77 ± 0.16 mm. These changes were both statistically significant ($P < 0.001$).

DISCUSSION

These experiments show that refilling the pig lens capsule with silicone oil to the same thickness as before surgery resulted in significant changes in the optical properties of the lens. First, the lens power (comparison A) and the lens radii of the refilled lens (comparison E) were lower than those of the natural lens. One would expect a higher lens power when the sphericity of the lens increases. This contradictory relationship can be explained by the lower refractive index of the refill material. The material used in our experiments was made with the intention of refilling human lenses, which have a lower equivalent refractive index than pig lenses. Second, there was a change in the sign of the spherical aberration of the lens from negative (−3.6 ± 2.0 D) to positive (7.9 ± 2.3 D; comparison A). This change can be explained by the replacement of the gradient refractive index in the natural lens by the homogeneous refractive index in the refilled lens. Comparison C showed that even if the lens contours are identical, the change from a gradient refractive index to a homogeneous refractive index results in a significant increase in spherical aberration. Third, the sphericity of the lens contours increases after refilling (comparison E). This could also be responsible for the increase in spherical aberration. However, comparison D showed that the increase in sphericity of the refilled lenses did not influence spherical

TABLE 1. Lens Powers and Spherical Aberrations of the Natural and Refilled Lenses

	SLRT		MRT	
	Lens Power	**Spherical Aberration**	**Lens Power**	**Spherical Aberration**
Natural pig lens	49.9 ± 1.5D	−3.6 ± 2.0D	49.9 ± 1.6D	11.0 ± 2.1D
Refilled pig lens	36.8 ± 1.5D	7.9 ± 2.3D	36.7 ± 1.6D	8.6 ± 1.4D

Data are the mean ± SD, as measured by SLRT and of the photographed contours of the natural and refilled lenses as measured by MRT.

aberration significantly, even though the same homogeneous refractive index was used.

One must remember that the lenses used in these experiments were removed from the eye. It is quite plausible that this had some influence on our data, especially if one considers the 0.4 ± 0.1-mm increase in mean natural lens thickness when the lens was removed from the intact pressurized eye and mounted in a plastic ring without stretching (Fig. 3). To estimate the changes in anterior lens curvature after an increase in lens thickness of 0.4 mm, we performed a calculation. The radius of the anterior lens curvature appeared to decrease from 11.1 to 7.0 mm (Appendix). This means that our conclusions are based on experiments with pig lenses with experimentally induced decreased radii of the lens curvatures. Under our experimental conditions, the change from a gradient refractive index to a homogeneous refractive index had the largest effect on spherical aberration. Even though the refractive index of the lens did not change, the additional changes in lens curvature due to refilling only resulted in a 2.0 ± 2.5 D ($P = 0.08$) change in spherical aberration.

The changes in spherical aberration in our experiments were assessed by directing parallel rays at the samples. In the real-eye situation, the cornea converges these parallel rays. To estimate this effect on the spherical aberrations in our experiments, we performed some calculations on an eye model in which the cornea was represented by an ideal lens with a power of 40 D and placed 4.2 mm in front of the lens. Under all four conditions, the resultant spherical aberrations in this "real eye" were approximately 40% of the values reported in Table 1.

Another item of consideration is that our conclusions were based on a comparison between the direct measurement of lens power and spherical aberration using SLRT and the lens power and spherical aberration calculated using MRT of the fitted surfaces derived from lens surface contour photography. The latter method may be sensitive to errors resulting from improper fit. Comparison B compared the datasets of refilled pig lenses measured by SLRT and by MRT. Because a refilled pig lens has a homogeneous refractive index, the two datasets should not differ significantly from each other. This was confirmed by our results and shows that the MRT method does not induce significant systematic errors.

Refraction of the eye will be the preferred endpoint for lens-refilling in a clinical setting. In the present study, however, the endpoint for refilling was the same axial thickness as before refilling. Koopmans et al.[12] showed that a 100%-refilled pig lens correlates with a lens thickness of approximately 7.0 mm. A change in mean lens thickness of 0.54 ± 0.16 mm (±SD) results in a change in lens power of 1 D, which is the predictive error of biometry in conventional cataract surgery in 85% of all cases.[15] Measurement of axial lens thickness with A-scan ultrasonography has an accuracy of ±0.1 mm and should, therefore, be an accurate endpoint for refilling. Moreover, it is easy to perform.

In human eyes, spherical aberration and the possibility of correcting it have received considerable attention recently.[16–18] It is the third major type of aberration after sphere and cylinder aberrations. Spherical aberration of the eye increases depth of focus, but decreases modulation transfer at high spatial frequencies at optimum focus.[19] Correcting spherical aberration in pseudophakic patients by implanting an intraocular lens with an aspheric design results in an increase in contrast sensitivity at optimum focus.[20–22] These influences of spherical aberration on the optical performance of human eyes make it relevant to predict the effect of lens refilling on this parameter. Based on our experiments and previous studies,[7,12] it can be concluded that there is an increase toward a positive value of spherical aberration after lens refilling. It is not clear, however, whether lens refilling in human eyes will result in the same large changes in spherical aberration seen in pig eyes. Pig lenses differ considerably from human lenses. They are more spherical and thicker than human lenses. It could be that the contributions of the gradient refractive index and the surface curvatures to the total amount of spherical aberration differ between the two species.

Jones et al.[23] showed that the refractive index profile in the central region of the human lens becomes flatter with age. Consequently, the spherical aberration changes from negative to positive when the human lens ages. Our refilled lenses had a homogeneous refractive index with a positive spherical aberration, quite similar to the optical qualities of an older lens. Therefore, it can be expected that refilling the lens in a younger individual induces a larger change in positive spherical aberration of the eye than in an older individual.

In conclusion, we found that refilling pig lenses with the silicone oil used in these experiments resulted in an increase in spherical aberration. The change from a gradient refractive index to a homogeneous refractive index played an important role. The change in lens curvatures after refilling did not result in a significant increase in spherical aberration. The influence of lens refilling on the spherical aberration of human lenses has to be determined by similar experiments in human eyes.

Appendix

To estimate the effect of a change in lens thickness on the anterior lens radius, the pig lens was represented as an intersection of two spheres. The volume of such an intersection is given by:

$$\frac{\pi(R + r - d)^2(d^2 + 2dr - 3r^2 + 2dR + 6rR - 3R^2)}{12d}$$

where R is the radius of the first sphere, r is the radius of the second sphere, and d is the distance between the center of the two spheres, which is calculated by $R + r$ − lens thickness.[24]

After the lens thickness was changed from 7.0 to 7.4 mm, the Goal-Seek Function in Excel (Microsoft, Redmond, WA) was used to find the anterior radius that would result in a lens with the same volume. To estimate the change in the anterior radius, we assumed that the posterior radius did not change with a change in lens thickness, as described by Koopmans et al.[25]

This calculation showed that a change in lens thickness from 7.0 to 7.4 mm resulted in a change of the anterior radius from 11.1 to 7.0 mm.

References

1. von Helmholtz H. *Handbuch der Physiologischen Optik.* Hamburg/Leipzig: Verlag von Leopold Voss; 1909.
2. Pau H, Kranz J. The increasing sclerosis of the human lens with age and its relevance to accommodation and presbyopia. *Graefes Arch Clin Exp Ophthalmol.* 1991;229:294–296.
3. Heys KR, Cram SL, Truscott RJW. Massive increase in the stiffness of the human lens nucleus with age: the basis for presbyopia? *Mol Vis.* 2004;10:956–963.
4. Fisher RF. The elastic contents of the human lens. *J Physiol (Lond).* 1971;212:147–180.
5. Glasser A, Campbell M. Presbyopia and the optical changes in the human crystalline lens with age. *Vision Res.* 1998;38:209–229.
6. Kessler J. Experiments in refilling the lens. *Arch Ophthalmol.* 1964;71:412–417.
7. Koopmans SA, Terwee T, Barkhof J, et al. Polymer refilling of presbyopic human lenses in vitro restores the ability to undergo

accommodative changes. *Invest Ophthalmol Vis Sci*. 2003;44: 250–257.

8. Nishi O, Nishi K. Accommodation amplitude after lens refilling with injectable silicone by sealing the capsule with a plug in primates. *Arch Ophthalmol*. 1998;116:1358–1361.
9. Nishi O, Hara T, Hara T, et al. Refilling the lens with an inflatable endocapsular balloon: surgical procedure in animal eyes. *Graefes Arch Clin Exp Ophthalmol*. 1992;230:47–55.
10. Hettlich HJ, Lucke K, Asiyo-Vogel M, et al. Lens refilling and endocapsular polymerization of an injectable intraocular lens: in vitro and in vivo study of potential risks and benefits. *J Cataract Refract Surg*. 1997;20:115–123.
11. Smith G, Atchinson DA, Pierscioneck BK. Modeling the power of the aging human lens. *J Optical Soc Am*. 1992;9:2111–2117.
12. Koopmans SA, Terwee T, Haitjema HJ, et al. Relation between injected volume and optical parameters in refilled isolated porcine lenses. *Ophthalmol Physiol Opt*. 2004;24:572–579.
13. Jantzen J-P, Hennes HJ, Rochels R, et al. Deliberate arterial hypotension does not reduce intraocular pressure in pigs. *Anesthesiology*. 1992;77:536–540.
14. Giers U, Epple C. Comparison of A-scan device accuracy. *J Cataract Refract Surg*. 1990;16:235–242.
15. Haigis W, Lege B, Miller N, et al. Comparison of immersion ultrasound biometry and partial coherence interferometry for intraocular lens calculation according to Haigis. *Graefes Arch Clin Exp Ophthalmol*. 2000;238:765–773.
16. Guirao A, Redondo M, Geraghty E, et al. Corneal optical aberrations and retinal image quality in patients in whom monofocal intraocular lenses were implanted. *Arch Ophthalmol*. 2002;120: 1143–1151.
17. Yoon G, MacRae S, Williams DR, et al. Causes of spherical aberration induced by laser refractive surgery. *J Cataract Refract Surg*. 2005;31:127–135.
18. Hersh PS, Fry K, Warren Blaker J. Spherical aberration after laser in situ keratomileusis and photorefractive keratectomy: clinical results and theoretical models of etiology. *J Cataract Refract Surg*. 2003;29:2096–2104.
19. Nio YK, Jansonius NM, Fidler V, et al. Spherical and irregular aberrations are important for the optimal performance of the human eye. *Ophthalmic Physiol Opt*. 2002;22:103–112.
20. Packer M, Fine H, Hoffman RS, et al. Prospective randomized trial of an anterior surface modified prolate intraocular lens. *J Refract Surg*. 2002;18:692–696.
21. Piers P, Fernandez EJ, Manzanera S, et al. Adaptive optics simulation of intraocular lenses with modified spherical aberration. *Invest Ophthalmol Vis Sci*. 2004;45:4601–4610.
22. Mester U, Dillinger P, Anterist N. Impact of a modified optic design on visual function: clinical comparative study. *J Cataract Refract Surg*. 2003;29:652–660.
23. Jones CE, Atchison DA, Meder R, et al. Refractive index distribution and optical properties of the human lens measured using magnetic resonance imaging (MRI). *Vis Res*. 2005;45:2352–2366.
24 MathWorld, a free resource from Wolfram Research, Champaign, IL; http://mathworld.wolfram.com/Sphere-SphereIntersection.html.
25. Koopmans SA, Terwee T, Haitjema HJ, et al. Effect of infusion bottle height on lens power after lens refilling with and without a plug. *J Cataract Refract Surg*. 2003;29:1989–1995.